Glycoconjugate Journal 18, 547–556, 2001
© 2002 Kluwer Academic Publishers. Manufactured in The Netherlands.

# Glycosylated molecular variants of C-reactive proteins from the major carp *Catla catla* in fresh and polluted aquatic environments

Indrani Paul[1], Chhabinath Mandal[2], Anthony K. Allen[3] and Chitra Mandal[1]*

[1] *Immunobiology,* [2] *Protein Design and Engineering Divisions, Indian Institute of Chemical Biology, Calcutta 700 032, India,* [3] *Molecular Pathology Section, Division of Biomedical Science, Imperial College School of Medicine, South Kensington, London SW7 2AZ, UK*

**Elevated level of pollutant specific glycosylated molecular variants of C-reactive protein have been purified to electrophoretic homogeneity from the sera of major carp, *Catla catla* confined in freshwater ($CRP_N$) and water polluted with nonlethal doses of cadmium ($CRP_{Cd}$), mercury ($CRP_{Hg}$), phenol ($CRP_{Ph}$) and hexachlorocyclohexane ($CRP_{Hex}$). These CRPs differ amongst themselves in electrophoretic mobility, and in their carbohydrate content ranging from 20–50%. CRPs interact with pneumococcal C-polysaccharide (CPS) showing different binding constants. Both phosphorylcholine (PC) and calcium are indispensable for binding. Studies on amino acid compositions, electrophoretic analysis, isoelectric focusing, binding to PC & CPS and secondary structures of the purified CRPs indicate, that, they differ from each other. However, they share the common properties of a CRP, including pentraxin structure revealed by electron microscopy. Taken together, our results provide a new structural insight regarding the connection between the presence of unique molecular variants and probably the toxicity therein combated.**

***Keywords:*** **C-reactive protein, aquatic pollution, sweet water fish, *Catla catla*, molecular variants**

***Abbreviations:*** **CRP, C-reactive protein; PC, phosphorylcholine chloride; CPS, pneumococcal C polysaccharide; EDTA, ethylene diamine tetra acetic acid; BSA, bovine serum albumin; HRP, horseradish peroxidase; ELISA, enzyme linked immunosorbent assay; DAB, 3,3′-diaminobenzidine; ABTS, 2,2′-azino-bis(3-ethylbenzthiazoline-6-sulfonic acid) diammonium salt; CD, circular dichroism.**

## Introduction

C-reactive proteins (CRPs), the prototypic acute phase protein are characterized by their ability to precipitate with pneumococcal C-polysaccharide (CPS) through phosphorylcholine (PC) moiety in a calcium dependent manner [1]. They belong to a phylogenetically ancient super-family of proteins termed 'pentraxins' consisting of non-covalently linked subunits arranged in a flat planer disc of pentameric symmetry. CRPs are normal constituents (0.05–4 mg/ml) in wide variety of species [2–10] including fresh water fishes. The CRP levels in fishes are increased by toxic agents [4–8] suggesting their role in host defense mechanism. In contrast, CRP is present in trace amounts (0.0001–0.0005 mg/ml) in almost all mammals [1,9,10]. Because of its 1000 fold increase within 24 hour after tissue damage, chemical trauma, intoxication, infection, injury and certain chemical stress, the human CRP is probably the single most useful molecule for monitoring acute phase reactions while primary function still remains unclear [9,10].

Intensive industrialization and agricultural improvement have resulted in a potential threat to the aquatic ecosystem [11, 12]. Several environmental pollutants are reported to induce a modest level of CRP in fresh water fish [4–7], yet, the existence of any relationship between the structural aspect of the CRPs induced and the stimulating agents by which it is induced has not been investigated in great details. Realizing this long-standing gap in our knowledge, we had addressed this point and reported that unique pollutant specific molecular variants of CRP are induced in the sera of *C. catla* in response to various pollutants as compared to normal aquatic conditions [4]. Most importantly, during the acute phase response distinct pollutant specific glycosylated molecular variants of fish CRP appear in a specific time dependent manner and coexist with the normal

*To whom correspondence should be addressed: Chitra Mandal, Immunobiology Division, Indian Institute of Chemical Biology, 4 Raja S.C. Mullick Road, Jadavpur, Calcutta 700 032, India. Tel.: 91-33-473-3491, 91-33-473-0492; Fax: 91-33-473-0284, 91-33-473-5197; E-mail: cmandal@iicb.res.in, Chitra_mandal@yahoo.com

form around the peak of induction though appearing as a single entity at the peak level [4]. These molecular variants appear possibly due to the differences in their glycan part [4–6] and contribute towards the variable lectin like properties, as reflected in their differential sugar binding characteristics [7].

In the light of these findings, these data has led us to certain pertinent questions. Does any correlation exist between individual pollutants and CRP at the molecular level? Are there any structural differences amongst these CRP molecules? Can these differences be correlated to their biological functions? The answer to these important questions might lead to the understanding of the mechanism of action of this group of acute phase proteins. The structure-function relationship of fish CRPs in response to various industrial effluents may serve as a biochemical model system for studying artificially elevated toxic aquatic ecosystem. Their nature and level of induction may be used as potential indicators of acute stress in aquatic animals.

In order to understand the nature of these CRP variants we have investigated the affinity purified CRPs from the serum of the freshwater fish, *C. catla* with biochemical, physicochemical and immunochemical means. In this communication the focus is on the extensive *in vitro* comparative characterization of the different glycosylated molecular variants of CRP under normal and toxic conditions. Importantly, our studies indicate that all the CRP variants markedly differ in their carbohydrate and amino acid compositions, isoelectric points and secondary structures thus opening a new set of questions and investigations.

## Materials and methods

### Purification of CRPs

*C. catla* were acclimatized at standard temperature, light and food in fish tanks. In different groups of fishes ($n = 10$) were exposed to $HgCl_2$ (0.1 ppm) or hexachlorocyclohexane (3.7 ppm), $CdCl_2$ (60 ppm) or phenol (10 ppm) separately to 3, 6, 12, 24, 36, 48, 72 hours. Control sets of fishes ($n = 10$) were kept in fresh water. $CRP_N$, $CRP_{Hg}$, $CRP_{Hex}$, $CRP_{Cd}$, and $CRP_{Ph}$ were purified from the sera of fishes confined in freshwater and polluted water at their peak time of induction namely 12, 12, 24, 48 hours respectively [4]. In brief, fish serum following 80% saturated ammonium sulphate precipitation was fractionated using Sepharose –PC affinity column pre-equilibrated with buffer A (0.05 M Tris buffered/HCl/0.15 M NaCl, pH 7.9, 0.02% sodium azide) with 0.01 M $Ca^{2+}$. The bound protein was eluted with 0.025 M PC in buffer A. The affinity purified CRP was dialyzed against buffer A and stored in aliquots at $-20^{\circ}$C. Proteins were estimated using BSA as standard [13]. The purity of CRPs was further checked by HPLC using a gel filtration column.

### Non-denaturing, SDS/PAGE and Western blot analysis

Nondenaturing PAGE (7.5%) [14] of purified CRPs were electrophoresed, electroblotted onto nitrocellulose [15] blocked with 1% BSA and incubated overnight with polyclonal anti-$CRP_N$ antibodies raised in rabbit [4] (diluted 1:200 in TBS-Tween 20, 0.001% BSA, pH 7.9). The antigen-antibody complex was detected using HRP conjugated goat anti-rabbit IgG (diluted 1:2,000) with a chromogenic substrate DAB.

CRPs (10 $\mu$g) before and after deglycosylation were analyzed by SDS-PAGE (15%) [16]. The gels were stained with Coomassie Brilliant Blue R-250. The apparent molecular weights were determined from the standard plot using known molecular weight markers. CRPs were deglycosylated with trifluoromethane sulphonic acid [4].

### Quantitation of CRPs in crude serum by sandwich ELISA

CRP levels in the crude serum were measured by sandwich ELISA in which the microtiter plates were coated with polyclonal murine anti-$CRP_N$ antibodies (50 $\mu$l/well) in coating buffer (0.05 M carbonate/bicarbonate buffer, pH 9.6). After washing with buffer A containing 0.05% Tween-20, 0.01 M $CaCl_2$ and 0.001% BSA and blocking with BSA (1% w/v), serum sample (50 $\mu$l/well) were added, incubated overnight at 4°C followed by washings. Rabbit anti-$CRP_N$ (1:1000) was added, incubated overnight at 4°C and washed thoroughly. The binding assayed by HRP-conjugated goat anti-rabbit IgG (1:5000) with a chromogenic substrate, ABTS and read at 405 nm by a microtitre plate spectrophotometer (Lab System Multiskan, MS). Experiments were repeated four times, each time in triplicate.

### Calcium-dependent CRP-PC binding

CRPs (6 $\mu$g/20 $\mu$l) were iodinated separately with $Na^{125}I$ [17] and purified through a Biogel P-10 column. For examination of $Ca^{2+}$-dependency of CRP-PC binding, fixed amount of iodinated CRPs were separately incubated with Sepharose-PC (20 $\mu$l) and different concentrations of $CaCl_2$ (0–100 mM) overnight at 4°C. After repeated washing with buffer A, pellets were centrifuged and bound CRPs were monitored in a gamma counter. Experiments were done in quadruplets. Controls were set up replacing $CaCl_2$ by equal volume of same buffer. Bound CRP was plotted against $CaCl_2$ (mM) added to calculate the amount of $Ca^{2+}$ needed for 50% saturated binding.

### CRP-CPS binding by ELISA

The binding of purified CRPs to CPS was tested by incubating various concentrations of CRP (0–4 $\mu$g in 50 $\mu$l) on CPS (200 ng/50 $\mu$l of coating buffer) coated plates for overnight at 4°C. The plate was, extensively washed and probed with rabbit anti- $CRP_N$ (diluted 1000 fold) using HRP color development system as described above.

Quantitation of bound CRP for Scatchard analysis [18] was obtained from a separate experiment in which CRPs in serial dilution (0–4 $\mu$g) were coated on to microtitre plates and color developed was measured as mentioned above. Linear portions of the plot of $OD_{405}$ vs CRP concentration obtained from these

direct binding experiments were used for calculating bound CRP at a titration point of CPS-CRP binding.

The specificity of CPS binding inhabitable by PC was studied by competition-inhibition ELISA. Fixed amounts (0.85 $\mu$g in $\mu$g/well) of $CRP_N$, $CRP_{Cd}$ or $CRP_{Hg}$ in separate experiments were added to the CPS (200 ng/well) coated plates in presence of varying concentration of PC (0–0.5 M) in buffer A with 0.01 M $Ca^{2+}$. The plates were treated and read as described above. Each experiment was done in triplicate.

### Metal analysis by atomic absorption spectroscopy

Quantification of metals of the purified CRPs was performed by atomic absorption spectrophotometer (Perkin-Elmer Model 3280) for the detection of any associated $Ca^{2+}$, $Cd^{2+}$, $Cu^{2+}$, and $Hg^{2+}$.

### Analytical isoelectric focussing

Analytical isoelectric focusing [19] of $CRP_N$, $CRP_{Cd}$ and $CRP_{Hg}$ (10 $\mu$g each purified at their peak level) were carried out on LKB ampholine polyacrylamide gel-(PAG) plates in the pH range 3–7 under native conditions according to the manufacturer's instructions (LKB Instruments Ltd., London). The isoelectric point (pI) was determined as a function of their migration from the cathode using proteins with known pI values (Sigma).

### Determination of molecular mass by Native PAGE

A series of native gels with 5%, 6%, 7.5%, 8%, 10% and 12% polyacrylamide were performed [14] with affinity purified $CRP_N$, $CRP_{Cd}$ and $CRP_{Hg}$ along with the standard molecular weight markers: $\alpha$-lactalbumin (14.2 kDa), carbonic anhydrase (29 kDa), chicken egg albumin (45 kDa), BSA (66, 132 kDa) and Jackbean urease (272, 545 kDa). Gels were fixed and stained for protein. Data were used for the determination of the native molecular weights of the CRPs [20]. This method uses the 'Ferguson plots' to discriminate among charge isomers, molecular isomers and forms which differ with respect to both charge and size, as well as to estimate molecular weight of a multimeric protein.

### Electron microscopy

$CRP_N$ in buffer A was applied to hydrophilic carbon membranes supported on copper grids. Negative staining was carried out with uranyl acetate as described [21]. Molecules were examined and photographed at a magnification of 60,000× with an electron microscope (JEM-100CX).

### Determination of amino acid compositions

Amino acid analyses were performed [22] on a Pharmacia-LKB amino acid analyzer. Hydrolysis was done in 6 M HCl under $N_2$ for 24 h at 110°C with Norleucine as the internal standard. Half-cystine values were obtained from samples, which had been previously oxidized with performic acid. Tryptophan was determined as described by Bredderman [23]. Amino acid compositions were used to examine the relatedness of *C. catla* CRPs with other CRPs using $S\Delta Q$ indices [6] calculated using the following formula.

$$S\Delta Q = \sum_j (X_{i,j} - X_{k,j})^2$$

Where subscripts $i$ and $k$ denote two proteins being compared and $X_j$ denotes contents of each amino acid $j$ as percentage. A program (written in basic and runs on any IBM compatible PC) developed in our laboratory in which either composition or sequence of proteins could be given as input was used. Algorithms have been incorporated in the same program to calculate the molecular weight of a polypeptide subunit from amino acid compositions based on the principle of Delaage [24]. The validity of calculations were verified with polypeptides of known molecular weights and found to be in good agreement even after random errors to the extent of 10% were introduced to the calculated compositions of the amino acids [25].

### Fluorescence emission spectroscopy

Fluorescence spectra of CRPs (370 ug/ml in buffer A) were obtained in fluorescence spectrofluorimeter (Hitachi model F-4010, Japan) at 25°C with excitation at 280 nm and emission wavelength were recorded over the range of 300–400 nm.

### Circular dichroism (CD) analysis

The CD spectra of purified CRPs (0.5 mg/ml of Buffer A) were measured at 25°C in a cuvette of 1 mm path length and 3.0 ml capacity with a JASCO J720 recording spectropolarimeter over a range of 200–300 nm. Average of 5 scans were taken for every datum, each corrected by subtracting contribution from the buffer and expressed in terms of mean residue ellipticities [$\theta$] in degree $cm^2$ $dmol^{-1}$ taking 110 as the mean residue molecular weight. The percentage of $\alpha$-helix, $\beta$-sheet and random coil was calculated using a computer program of curve fitting based on minimum standard deviation developed by us [25] using the standard data [26]. The computer program generates a normalized plot of the $\theta$ values taking the observed range between 0 & 100%.

## Results

### Purified CRPs differ in electrophoretic mobilities but have crossreactive antigenic sites

The purified CRP from the sera of *C. catla* fishes confined in fresh as well as in polluted water, at their paek time of induction eluted as a single symmetrical peak by 25 mM PC-chloride from affinity chromatography on Sepharose-PC establishing the

purity of the protein samples. Elution of all the five CRPs from the same affinity matrix prompted us to test for their immunological crossreactivity. The polyclonal antisera prepared against anti-$CRP_N$ shows strong immunological crossreactivity as evidenced by western blot analysis on native PAGE of the five purified CRPs (Figure 1A). The presence of single band in each lane corresponds to the unique presence of five CRPs at their peak level (lanes 2–6). Lane 1 shows the electrophoretic mobility of $CRP_N$.

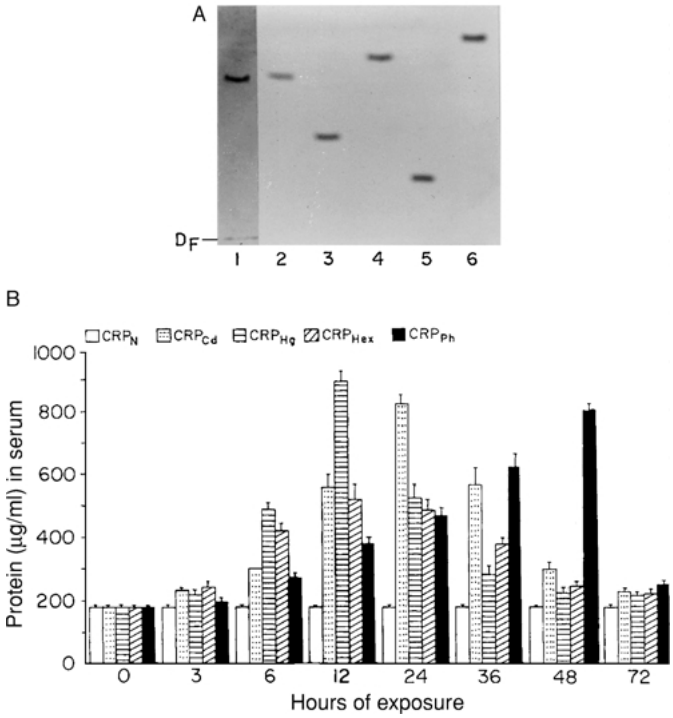


**Figure 1.** Qualitative and quantitative difference amongst CRP variants by western blot analysis. (A) Equal amounts (12 $\mu$g) of $CRP_N$ (lane 2), $CRP_{Cd}$ (lane 3), $CRP_{Hg}$ (lane 4), $CRP_{Hex}$ (lane 5) and $CRP_{Ph}$ (lane 6) were blotted onto nitrocellulose after native PAGE (7.5%) analysis. The primary antibody used was anti-$CRP_N$ (1:200 dilution). HRP conjugated goat anti-rabbit IgG (1:2,000) was used as secondary antibody. The antigen-antibody complexes were visualized by DAB. Lane 1 shows $CRP_N$ (12 $\mu$g) stained with Coomassie Blue. $D_F$ is the dye front. (B) Quantitation of CRP in serum by sandwich ELISA: *C. catla* was exposed for 0–72 h to $CdCl_2$ (60 ppm), $HgCl_2$ (0.10 ppm), hexachlorocyclohexane (3.70 ppm) and phenol (10 ppm) treated water as well as in fresh water. At each specified time point serum was collected and the level of CRPs was quantitated directly from crude serum by sandwich ELISA as described under "Materials and methods". Affinity purified $CRP_N$ was used as standard. The level of CRP in serum is plotted against the corresponding time of exposure (0–72 hr) for each pollutant. Normal level of CRP were determined from control sets at all the time points and plotted likewise. Means and standard deviations of eight independent experiments are shown.

Differences in serum CRP levels during acute phase response

Quantitation of the different extent of CRPs induced with increased duration of exposure of *C. catla* to all four different pollutants by sandwich ELISA (Figure 1B). All the pollutants affected the serum level differently both with respect to time course required to attain the peak of induction and the amount of total CRP present at these peak levels. Thus, CRPs behaved as an acute phase reactant with a maximum rise of about 5.0, 3.2, 4.6 and 4.5 folds compared to normal level in the sera of mercury, hexachlorocyclohexane, cadmium and phenol polluted fishes at 12 h, 12 h, 24 h and 48 h respectively. Considering the (i) doses, (ii) peak levels and (iii) kinetics of induction, mercury appears to be the strongest inducer. CRPs returned to normal level approximately after 48 h with cadmium, mercury and hexachlorocyclohexane and after 72 h with phenol.

CRP binding to PC is $Ca^{2+}$-dependent

The $Ca^{2+}$-dependent PC-binding activity is evident as different variants of CRP were purified from the PC affinity matrix. The concentration of $Ca^{2+}$ necessary for half maximal binding for $CRP_N$ as well as for the four variants was 2.25 mM. A representative profile of the binding of $CRP_N$ to Sepharose—PC with increasing concentration of $Ca^{2+}$ is depicted in Figure 2. In contrast, no binding was observed in the absence of $Ca^{2+}$ and binding was completely inhibited by EDTA (0.1 M).

Quantitation of the binding of CRP to CPS

Since all the CRPs showed characteristic $Ca^{2+}$-dependent binding to PC it prompted us to evaluate the binding properties of CRPs with CPS. Figure 3A shows the titration curve of

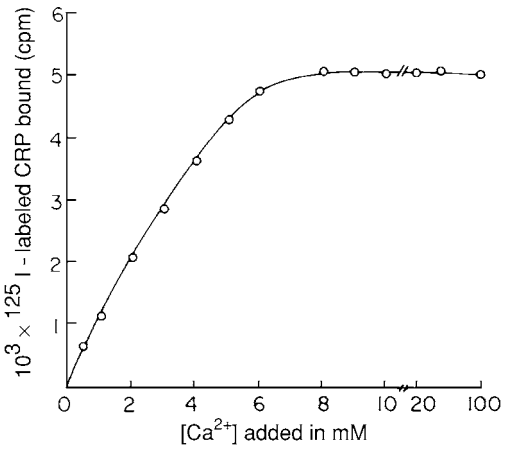


**Figure 2.** Calcium dependent binding of CRP to PC-affinity matrix. Increasing concentration of $Ca^{2+}$ (0–100 mM) was added to a fixed amount of a mixture of [$^{125}$I]-labeled CRP and PC-affinity matrix and incubated overnight at 4°C to effect binding. The mixtures were centrifuged, pellets were washed thrice and the readings (in CPM) were plotted against the concentration (mM) of $Ca^{2+}$ added.

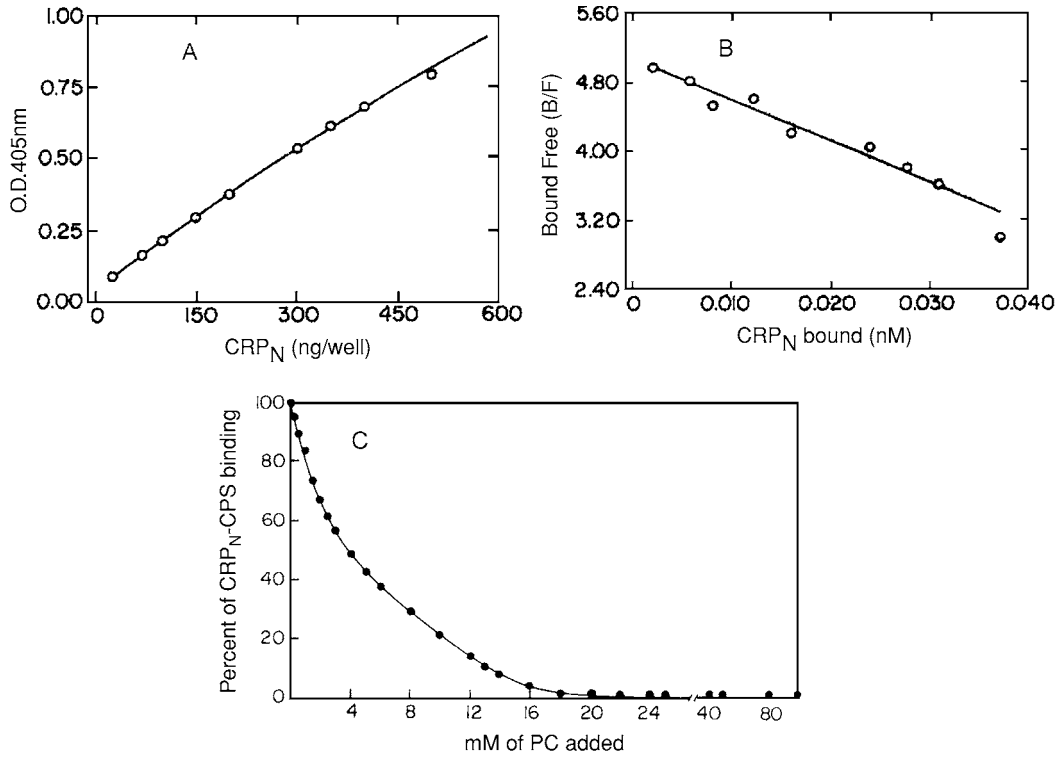


**Figure 3 (A and B).** Scatchard analysis and specificity of CRP-CPS binding. Fixed amounts of CPS (200 ng/50 $\mu$l) were coated on to the wells and titrated with varying concentrations of CRP (0–4 $\mu$g/50 $\mu$l). Bound CRP were measured and plotted as a function of its concentration (A), in which the circles are the experimental points and the solid line is the binding curve calculated from the apparent association constant obtained from the Scatchard plot (B) in which bound/free CRP has been plotted against bound CRP (nM). Correlation between color densities and the concentration was obtained from a separate experiment in which varying amounts of CRP (0–4 $\mu$g) was coated. (C) Inhibition of CPS-CRP binding with PC by competition ELISA. On a CPS (200 ng) coated ELISA plate, a fixed concentration of CRP (850 ng/50 $\mu$l) in buffer A along with varying concentrations of PC (0–0.5 M) was incubated. Bound CRP was measured at 405 nm and the extent of inhibition (%) has been plotted as a function of PC concentration.

CPS with varying amounts of $CRP_N$ and the corresponding Scatchard plot is shown in Figure 3B. The apparent binding constants ($K_a$) of $CRP_N$, $CRP_{Cd}$ and $CRP_{Hg}$ to CPS were found to be $4.82 \times 10^{10}\,M^{-1}$, $3.27 \times 10^{10}\,M^{-1}$ and $5.23 \times 10^{10}\,M^{-1}$ respectively indicating that the strength of binding vary significantly.

## CRP-CPS binding is inhibited by PC

The specificity of CRP towards the PC moiety of CPS was confirmed by competition ELISA Figure 3C, which shows the percent of binding inhibited with increasing amounts of PC. The binding was fully inhibited by 20 mM PC with a $IC_{50}$ value of 3.75 mM. Since PC inhibited the binding of CRP to CPS, it is clear that the binding is through the PC residues of CPS.

## Non-existence of metal ion(s) in purified CRPs

On marking the electrophoretic differences between the three CRP variants the natural query that arose was if this difference was due to association of metal ions with the induced CRPs. Atomic absorption spectroscopic results indicate that no significant amount of metal e.g., $Ca^{2+}$, $Cd^{2+}$, $Cu^{2+}$, and/or $Hg^{2+}$ were present in the CRP variants in either bound or associated state.

## Analysis of charge heterogeneity by Isoelectrofocusing (IEF)

Since metal ion chelation is not the governing factor for different electrophoretic mobilities we went on to investigate if heterogeneity in charge was due to the induced CRPs as compared to $CRP_N$. Affinity purified $CRP_N$, $CRP_{Hg}$ and $CRP_{Cd}$ produced reproducible pattern of single sharp band at pH 5.06, 4.90 and 4.82 respectively in IEF gel (Figure 4) reflecting the existence of a single molecular entity of CRP at the peak level.

## Variation in the molecular weight in CRPs

The variation in their carbohydrate contents [4] and now in their pI values led us to investigate for differences in the molecular weights of the purified $CRP_N$, $CRP_{Cd}$ and $CRP_{Hg}$. Due to the high content of carbohydrates, the molecular mass was determined by various means. $CRP_N$ with HPLC retention time of 8.6 estimated to a molecular mass of 199.5 kDa when plotted on

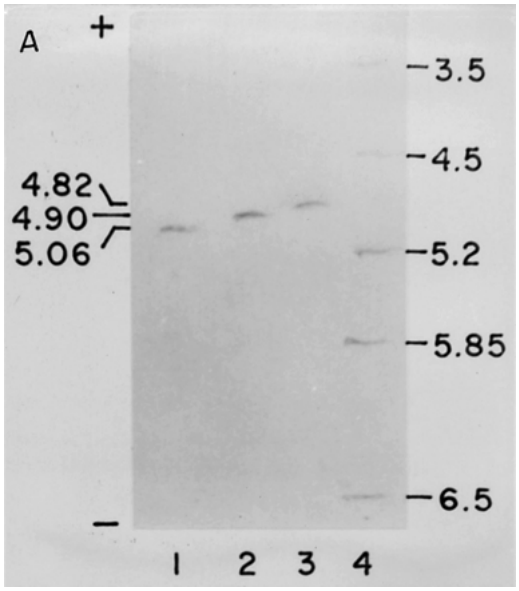


**Figure 4.** Isoelectric focusing of CRPs. Experiments were carried out by applying 10 $\mu$g of purified $CRP_N$ (lane 1), $CRP_{Hg}$ (lane 2) and $CRP_{Cd}$ (lane 3) in a pH gradient 3–7 as described under Material and methods. The gels were stained with Coomassie Blue. Standard markers are in lane 4.

the standard curve (figure not shown). Electrophoretic method showed the corresponding molecular mass values for whole $CRP_N$, $CRP_{Cd}$ and $CRP_{Hg}$ as 272, 266 and 287 kDa respectively. It may be noted that all three forms of the CRPs showed identical pentraxin structures under electron microscope (Figure 5A). No apparent differences were observed in the mobility of subunits in SDS-PAGE showing identical molecular mass of 22 kDa and 29 kDa (Figure 5B, lane 5–7).

Total carbohydrate contents of all CRPs were estimated spectrophometrically (at 490 nm) by the phenol sulfuric acid method and found to be 49.7%, 26.8% and 20.2% for $CRP_{Cd}$, $CRP_{Hg}$ and $CRP_N$ [4]. Interestingly, these CRPs after deglycosylation exhibited subunits of variable mass (Figure 5B, lanes 2–4) corresponding to 19.0 and 21.5 kDa for $CRP_N$ while subunits of $CRP_{Cd}$ were 16.0 & 18.5 kDa and for $CRP_{Hg}$, 18.0 & 21.5 kDa respectively. The completeness of deglycosylation was checked by DIG glycan detection kit [4]. Computational analysis of the amino acid composition of the three CRPs (excluding the carbohydrate content) revealed their subunit molecular weights as 21.6 and 28.8 for $CRP_N$; 15.5 and 19.8 for $CRP_{Cd}$ and 16.2 and 20.1 kDa for $CRP_{Hg}$ (Table 1).

## Analysis of purified CRPs from amino acid compositions

The differences in apparent molecular weight (Table 1) as well as the identical appearance of the three CRPs on electron microscopy (Figure 5A) appealed to us to compare their amino acid contents. From Table 2, it is apparent that small but significant differences exist between the individual amino acids of the three proteins. Although, all of them have fairly high content of

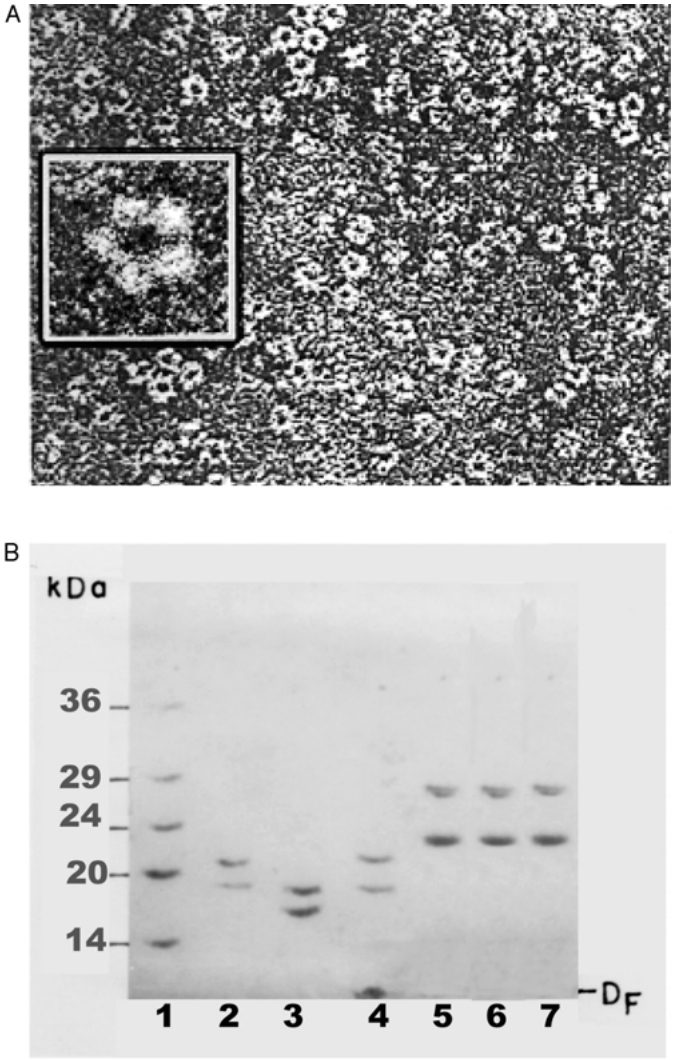


**Figure 5.** (A) Electron micrograph of $CRP_N$. Electron microscopic appearance of CRP molecules negatively stained with uranyl acetate on the carbon membrane showing pentagonal structure at a magnification of $\times$60,000. Inset. A single pentraxin structure of *C. catla* CRP with $C_5$ symmetry. (B) Analysis of glycosylated and deglycosylated CRPs on SDS-PAGE (15%). Standard protein markers are in lane 1. Lanes 2–7 represent 10 $\mu$g each of deglycosylated $CRP_{Hg}$, $CRP_{Cd}$, $CRP_N$ and glycosylated CRPs respectively.

acidic amino acids ($\sim$24% of the total), CRPs significantly vary in content of methionine ($CRP_{Hg} : CRP_{Cd}$: $CRP_N :: 8 : 5 : 1$), tryptophan ($CRP_N : CRP_{Cd} : CRP_{Hg} :: 1.6 : 1.4 : 1$) and cysteine $CRP_{Cd} : CRP_N : CRP_{Hg} :: 1.04 : 1 : 1.36$)

## Comparison with CRPs from other species by $S\Delta Q$ analysis

The amino acid compositions have been utilized to examine the relatedness among different forms of *C. catla* CRPs and CRP from other sources. It may be noted that $S\Delta Q$ value between

**Table 1.** Molecular mass of the subunits of CRPs in kilo daltons

| | *Subunit molecular mass (monomeric)* | | |
|---|---|---|---|
| | *SDS-PAGE analysis*[1] | | *From amino acid analysis*[2] |
| *CRP* | *Glycosylated* | *Deglycosylated* | *Deglycosylated* |
| $CRP_N$ | 22, 29 | 19, 21.5 | 21.6, 28.8 |
| $CRP_{Cd}$ | 22, 29 | 16, 18.5 | 15.5, 19.8 |
| $CRP_{Hg}$ | 22, 29 | 18.0, 21.5 | 16.2, 20.1 |

[1]SDS-PAGE analysis was carried out using glycosylated and deglycosylated CRPs according to method of Laemmli [16]. Relative electrophoretic mobilities of all three CRPs were plotted against specified standard markers. CRPs (200 $\mu$g) were deglycosylated with trifluromethane sulphonic acid [4].
[2]Calculated from amino acid compositions (Table 2) based on the principle of Delaage [24].

**Table 2.** Comparison of amino acid composition of *C. catla* CRPs

| | *mol %* | | |
|---|---|---|---|
| *Amino acid* | $CRP_N$ | $CRP_{Cd}$ | $CRP_{Hg}$ |
| Asp | 9.5 | 9.8 | 9.5 |
| Thr | 6.9 | 6.9 | 6.9 |
| Ser | 8.1 | 8.7 | 7.8 |
| Glu | 12.1 | 12.2 | 11.3 |
| Pro | 8.1 | 7.6 | 8.1 |
| Gly | 8.4 | 8.9 | 7.5 |
| Ala | 5.6 | 5.7 | 5.8 |
| 1/2 Cys[1] | 2.3 | 2.2 | 3.0 |
| Val | 6.3 | 5.9 | 6.4 |
| Met | 0.4 | 2.0 | 3.2 |
| Ile | 4.6 | 4.4 | 4.8 |
| Leu | 8.3 | 7.5 | 8.2 |
| Tyr | 3.2 | 3.4 | 3.3 |
| Phe | 3.5 | 3.3 | 3.5 |
| His | 2.6 | 2.3 | 2.1 |
| Lys | 4.9 | 4.3 | 4.1 |
| Trp[2] | 1.1 | 1.0 | 0.7 |
| Arg | 4.1 | 4.0 | 3.8 |

Amino acid analysis was performed on a Pharmacia-LKB amino acid analyzer [22]. The values were derived from an average of three hydrolysis in 6 M HCl for 24 h at 110°C. Norleucine was the internal standard.
[1]Determined separately as cysteic acid after hydrolysis of performic acid-oxidized sample.
[2]Determined spectrophotometrically [23].

$CRP_N$ and $CRP_{Cd}$ is very small (∼5) and that between $CRP_N$ and $CRP_{Hg}$ is also close (∼11) indicating very close relation between them in terms of amino acid composition (Table 3). From $S\Delta Q$ values *C. catla* CRPs also show close relatedness to the mammalian CRP, especially to mouse, rabbit and also to the CRP from the invertebrate, *Limulus polyphemus*. Though showing close relation to CRPs from other pisces yet it deviates significantly from rainbow trout CRP (∼141).

**Table 3.** $S\Delta Q$ values between the CRPs of *C. catla* and CRPs of other origin

| | $S\Delta Q$ | | |
|---|---|---|---|
| *Protein* | $CRP_N$ | $CRP_{Cd}$ | $CRP_{Hg}$ |
| *C. catla* $CRP_N$ | ... | 4.92 | 10.72 |
| *C. catla* $CRP_{Cd}$ | 4.92 | ... | 6.80 |
| *C. catla* $CRP_{Hg}$ | 10.72 | 6.80 | ... |
| Lumpsucker CRP | 55.83 | 50.02 | 54.11 |
| Plaice CRP | 69.60 | 75.39 | 71.00 |
| Dog fish CRP | 79.83 | 69.84 | 81.95 |
| Rainbow trout CRP | 141.79 | 137.76 | 149.53 |
| Rabbit CRP | 41.26 | 40.19 | 42.04 |
| Mouse CRP | 32.41 | 31.60 | 35.77 |
| Human CRP | 83.33 | 89.38 | 83.31 |
| *Limulus* CRP | 48.17 | 52.24 | 63.29 |

$S\Delta Q$ indices were calculated using the following formula.

$$S\Delta Q = \sum_j (X_{i,j} - X_{k,j})^2$$

Where subscripts *i* and *k* denote two proteins being compared and $X_j$ denotes contents of each amino acid *j* as percentage. Calculations were done using a program developed in our laboratory.

## Fluorescence emission measurement of CRPs

The differences in the tryptophan content of CRPs (Table 2) initiated the investigation of the fluorescence emission spectra of CRPs. All three forms gave emission maxima at 338 nm but interestingly the intensities at the maxima differ at the same concentration of the proteins in the following order $CRP_N > CRP_{Cd} > CRP_{Hg}$ in accordance with the tryptophan content of the three CRPs.

## Variation in secondary structures of CRPs

To examine if there is any variation in secondary structures of different forms of CRPs, CD spectra were recorded and analyzed for $\alpha$-helix, $\beta$-sheet and random coil conformations of the main chain. Panels a, b and c of Figure 6 present the experimental points along with the best fitted spectra for $CRP_N$, $CRP_{Cd}$ and $CRP_{Hg}$ respectively. The analyses of the secondary structures revealed 18, 29 and 24% $\alpha$-helix, 34, 32 and 29% $\beta$-structure and 48, 39 and 46% random coil for $CRP_N$, $CRP_{Cd}$ and $CRP_{Hg}$ respectively. It may be noted that the experimental values could be obtained only up to 210 nm for $CRP_{Cd}$ (Panel b) and 215 nm for $CRP_N$ and $CRP_{Hg}$ (Panel a & c). However, the calculated line has been drawn up to 190 nm, as the standard values are available in the literature [26].

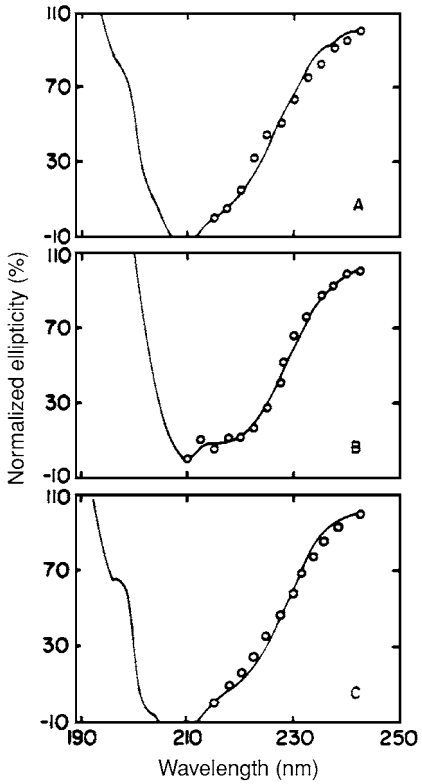


**Figure 6.** Circular dichroism Spectra of CRPs. Panels A, B and C are CD spectra of $CRP_N$, $CRP_{Cd}$ and $CRP_{Hg}$ respectively (1.2 mg/3 ml in 0.02 M Tris/HCl/0.15 M NaCl, pH 7.9) in far UV region at 25°C. The measured mean residue ellipticities were iteratively fitted with the varying percentages of secondary structures. After normalization, deviations were calculated for each step of iteration to obtain the best fit with the lowest deviation. The experimental values are shown as filled circles and the curve is the best fitted spectra.

## Discussion

Although the induction of CRP in acute phase response is well known it has not been studied in details at the molecular level. In case human CRP, potential pitfall is the induction from a very low basal level making it difficult to compare the differences between the normal and the induced forms. In *C. catla* the normal level is quite high (0.2 mg/ml) and is also inducible by a number agents [4]. Accordingly, this was selected as a model to examine the molecular nature of different forms of CRP.

The major finding of this investigation is that the normal form of CRP differs from the induced forms. The characterization of these CRPs by native western (Figure 1A), SDS-PAGE (Figure 5B), analytical IEF (Figure 4) and the molecular mass of the subunits (Table 1) revealed a variation in their chemical compositions. Most importantly, marked differences in electrophoretic mobilities of these CRPs (Figure 1A), gave the first indication that distinct chemical entities induced in a pollutant specific manner may arise with variation in the structure at molecular level. These differences in mobility may also be attributed to the presence of variable amino sugars as determined by the amino acid analyzer and neutral sugars by gas liquid chromatography [4]. Overall charge differences perhaps arise due to variable negatively charged sialic acid content as detected by DIG glycan differentiation kit and further quantitation by fluorimetric method [4]. It is worthwhile to point out that sialic acids are directly involved in many biological processes [27, 28]. Single band in Figure 1 indicate firstly, the purity of the CRPs to apparent homogeneity, secondly, the presence of similar antigenic sites on the five proteins, thirdly, their differences in electrophoretic migration and finally their existence as distinct and pollutant specific molecular entities.

The sharp and quick rise of CRP level, on exposure to various toxic substances, suggests that it may act as an autologous protective mechanism. Interestingly, though the dosage of the pollutants applied caused no mortality in the fish, elevated levels of CRP clearly serve as an index of internal damages. It implies a possible link between acute phase response and clearance of toxic substances. Doses of pollutants, peak levels of induction, and the circulatory life span of the CRPs vary significantly with types of pollutants (Figure 1B) implicating the necessity for the urgency of detoxification. The biological significance of this elevation for a short time due to systemic inflammatory response is not yet clearly understood. It may be envisaged that CRP needs different time and different amount for the clearance of the toxic pollutants depending on the degree of damage *in vivo*.

A single band of each purified CRP as observed by IEF (Figure 4) reconfirm the purity of the samples and thus reflecting the existence of a single molecular entity of CRP at the peak level. The CRP variants show slight differences in pI values, which indicate charge heterogeneity. This may be contributed by the acidic sugars e.g. sialic acids [4]. Pentraxins from other species always exhibit heterogeneity of pI [6, 29, 30]. Rainbow trout CRP shows a pI of 4.74 and whereas rat CRP is composed of closely spaced bands of pI between 3.8 and 4.0, goat CRP shows 5 closely spaced bands in pH range 6.65–7.0 and dog CRP exhibits 12 closely spaced bands (pI 5.6–6.65) and also an isolated single band at 5.3.

Structural variations in the forms of CRP are also reflected in their variable sulphur containing amino acids cysteine and methionine. $CRP_{Hg}$ contains 8 and 1.3 times more methionine and cysteine respectively compared to $CRP_N$ (Table 2). It may be envisaged that a mutation in the genomic structure or post translation deletion of C terminus are possibly responsible. Both cysteine and methionine are known to possess antioxidant properties due to their affinity for $Hg^{2+}$ preventing free radical production [31]. It may be extrapolated that $CRP_{Hg}$ probably binds to mercury through methionine and/or cycteine and thus prevents cell damage. Variations in tryptophan content are corroborated with the differences in intensity of fluorescence emission spectra.

Variation in molecular size has been repeatedly observed in SDS-PAGE and amino acid composition. The molecular masses of deglycosylated CRPs are in good agreement with the values

obtained from amino acid composition. Because of the high carbohydrate content, the subunit molecular mass may not be accurate due to anomalous behavior of glycoproteins in SDS-PAGE [32]. Simple arithmetic predicts glycosylated masses the two subunits around 24 & 27.7 for $CRP_{Cd}$, 22.8 & 27.2 for $CRP_{Hg}$ and 22.8 & 25.8 for $CRP_N$ respectively. For $CRP_{Hg}$ and $CRP_N$, the observed masses are in close agreement (atleast with 22 kDa), it is little high for $CRP_{Cd}$ as corroborated with its very high (49%) glycosylation. Similar differences in subunit molecular masses of glycosylated and deglycosylated forms have been reported in other CRPs [6, 33].

It may be highlighted that these notable differences in the electrophoretic mobility could be missed if only SDS-PAGE were carried out as all the induced glycosylated forms move to the same position (Figure 5B lane 5–7) but the differences are observed only in native PAGE. It may therefore be concluded that these differences are probably due to the cumulative effects of different types of amino acids, different percentages and types of sugars as the mobility of proteins in native gels are known to be affected by charge, mass and effective hydrodynamic shapes of the molecules. Interestingly, in spite of these unique differences, Figure 5A reveals that all CRPs are composed of five subunits (paired) per molecule where each unit of the pentraxin are formed by pairing of the two non-identical subunits as supported by the appearance of entirely single pentameric disc with no visual tendency to stack.

CD analysis revealed that all three glycosylated CRPs contained different amounts of $\alpha$-helix and $\beta$-sheet structures. Covalently linked carbohydrates are known to affect the secondary structures of a polypeptide. Accordingly, it may be postulated that the above differences in the main-chain conformations may be attributed to differences in the carbohydrate composition.

The $CRP_{Cd}$ and $CRP_{Hg}$ with $CRP_N$ showed complete immunological cross reactivity (Figure 1A) indicating that there are enough common epitopes on their surfaces, homologous region may be the $Ca^{2+}$ mediated PC binding regions. However, it would be interesting to identify different epitopes on different variants of the fish CRP, paving the way for the immunological detection of the different pollutants.

Taken together, our results strongly suggest that pollutant specific, unique, molecular variants of CRP, differing distinctly from each other in their chemical forms, are induced in serum on exposure to different environmental toxicants in a specific time dependent manner probably to combat the toxicity thus generated. Accordingly, our findings would stimulate intensive search for such type of agent specific induction of other CRPs of clinical importance. We propose that if such process were established in case of human CRP it would open up new avenues of research.

## Acknowledgments

We are thankful to Dr. Sailen Mookerjea of Memorial University of Newfoundland, Newfoundland, Canada for the gift of pneumococcal C-polysaccharide, Dr. A. Sen for his help in deglycosylation experiments and Mr. A. Mallick for his excellent technical assistant. I. P. was a Senior research fellow of the Council of Scientific and Industrial Research, India.

## References

1 Shrive AK, Cheetham GMT, Holden D, Myles DAA, Turnell WG, Volanakis JE, Pepys MB, Bloomer AC, Greenhough TJ, Three dimensional structure of human C-reactive protein, *Nature Struct Biol* **3**, 346–54 (1996) and references there in.

2 Armstrong PB, Swarnakar S, Srimal S, Misquith S, Hahn EA, Aimes RT, Quigley JP, A cytolytic function for a sialic acid binding lectin that is a member of the pentraxin family of proteins, *J Biol Chem* **271**, 14717–21 (1996) and references there in.

3 Mandal C, Biswas M, Nagpurkar A, Mookerjea S, Phosphoryl choline binding protein from the hemolymph of *Achatina fulica* snail, *Dev Comp Immunol* **15**, 227–39 (1991) and references there in.

4 Paul I, Mandal C, Mandal C, Effect of environmental pollutants on the C-reactive protein of a freshwater major carp, *Catla catla*, *Dev Comp Immunol* **22**, 519–32 (1998).

5 Sinha S, Mandal C, Microheterogeneity of C-reactive protein in the sera of fish *Labeo rohita* induced by metal pollutants, *Biochem Biophys Res Commun* **226**, 681–7 (1996).

6 Sinha S, Mandal C, Allen AK, Mandal C, Acute phase response of C-reactive protein (CRP) of *Labeo rohita* to aquatic pollutants is accompanied by the appearance of distinct molecular forms, *Archives Biochem Biophys* **396**, 139–50 (2001).

7 Mandal C, Sinha S, Mandal C, Lectin like properties and differential sugar binding characteristics of C-reactive proteins purified from sera of normal and pollutant induced *Labeo rohita*, *Glycoconjugate J* **16**, 741–50 (1999).

8 Maudsley S, Baltz ML, Munn EA, Buttress N, Herbert J, Feinstein A, Pepys MB, Isolation and characterization of goat C-reactive protein, *Biochem Biophys Acta* **924**, 75–80 (1987).

9 Volanakis JE, Human C-reactive protein: Expression, structure and function, *Mol Immunol* **38**, 189–97 (2001) and references therein.

10 Gabay C, Kushner I, Acute phase proteins and other systemic responses to inflammation, *The New Eng J Med* **340**, 448–54 (1999).

11 Hare L, Tessier A, Predicting animal cadmium concentration in lake, *Nature* **380**, 430–32 (1996).

12 Sellers P, Kelly CA, Rudd JWM, MacHutchon AR, Photodegradation of methylmercury in lakes, *Nature* **380**, 694–7 (1996).

13 Lowry OH, Rosebrough NJ, Farr AL, Randall RJ, Protein measurement with folin phenol reagent, *J Biol Chem* **193**, 265–75 (1951).

14 Davis BJ, Disc electrophoresis, II: Method and application to human serum protein, *Ann N Y Acad Sci* **121**, 404–27 (1964).

15 Towbin HT, Stackelin T, Gordon J, Electrophoretic transfer of proteins from polyacrylamide gels to nitrocellulose sheets: Procedure and some applications, *Proc Natl Acad Sci USA* **76**, 4350–4 (1979).

16 Laemmli UK, Cleavage of structural proteins during the assembly of the head of bacteriophage T4, *Nature* **227**, 680–5 (1970).

17 Hunter WM, *Handbook of Experimental Medicine*, edited by Weir DM (Blackwell, Oxford, 1978), pp. 14.1–14.3.

18 Scatchard G, The attraction of proteins for small molecules and ions, *Ann N Y Acad Sci* **51**, 660–72 (1949).

19 Rufo GA Jr, Singh JP, Babcock DF, Lardy HA, Purification and characterization of a calcium transport inhibitor protein from bovine seminal plasma, *J Biol Chem* **257**, 4627–32 (1982).
20 Bryan JK, Molecular weight of protein multimers from polyacrylamide gel electrophoresis, *Anal Biochem* **78**, 513–19 (1977).
21 Stroud RM, Shin HS, Shelton E, In *Methods in Molecular Biology*, edited by Zockaria TP, Vol. 4 (Marcel Dekker, New York, 1973), pp. 194–205.
22 Basu S, Mandal C, Allen AK, Chemical-modification studies of a unique sialic acid binding lectin from the snail *Achatina fulica*, *Biochem J* **254**, 195–202 (1988).
23 Bredderman PJ, Tryptophan analysis of proteins in 6 M guanidine hydrochloride: Modification for more general application, *Anal Biochem* **61**, 298–301 (1974).
24 Delaage M, Sur la recherche du poids moleculaire le plus coherent avec l'analyse des acides amines d'une proteine, *Biochim Biophys Acta* **168**, 573–5 (1968).
25 Mazumdar A, Chatterjee R, Adak S, Ghosh A, Mandal C, Banerjee R, Characterization of sheep lacrimal peroxidase and its major physiological electron donor, *Biochem J* **314**, 413–9 (1996).
26 Chen Y-M, Yang JT, Chau KH, Determination of the helix and $\beta$-form of proteins in aqueous solution by circular dichroism, *Biochemistry* **13**, 3350–9 (1974).
27 Sharma V, Chatterjee M, Sen G, Ch. A Kumar, Mandal C, Role of specific 9-O acetylated sialoglycoconjugates in activation of the alternate complement pathway in mammalian erythrocytes, *Glycoconjugate J* **17**, 859–83 (2000) and references therein.
28 Chatterjee M, Sharma V, Mandal C, Sundar S, Sen S, Identification of antibodies directed against O-Acetylated sialic acids in visceral leishmaniasis: Its diagnostic and prognostic role, *Glycoconjugate Journal* **15**, 1139–45 (1998).
29 Murai T, Kodama H, Naiki M, Mikami T, Izawa H, Isolation and characterization of rainbow trout C-reactive protein, *Dev Comp Immunol* **14**, 49–58 (1990).
30 De Beer BC, Baltz ML, Munn EA, Feinstein A, Taylor J, Bruton C, Clamp JR, Pepys MB, Isolation and characterization of C-reactive protein and serum amyloid P component in the rat, *Immunol* **45**, 55–70 (1982).
31 Martin Mateo MC, Aragon P, Prieto MP, Inhibitory effect of cysteine and methionine on free radicals induced by mercury in red blood cells of patients undergoing haemodialysis, *Toxicol in vitro* **8**, 597–9 (1994).
32 Segrest JP, Jackson RL, Molecular weight determination of glycoproteins by polyacrylamide gel electrophoresis in sodium dodecyl sulphate, *Methods Enzymol* **28**, 54–63 (1972).
33 Yang C, Mookerjea S, Nagpurkar A, Clearance of rat C-reactive protein *in vivo* and by perfused liver, *Glycobiology* **2**, 41–48 (1992).

Received 27 November 2001; revised 17 May 2002;
accepted 17 May 2002